ELSEVIER

International Journal of Mass Spectrometry 195/196 (2000) 419–437

International Journal of Mass Spectrometry

Ion trap collisional activation of protonated poly(propylene imine) dendrimers: generations 1–5

Scott A. McLuckey*, Keiji G. Asano, T. Gregory Schaaff, James L. Stephenson Jr.

Chemical and Analytical Sciences Division, Oak Ridge National Laboratory, Oak Ridge, TN 37831-6365, USA

Received 7 June 1999; accepted 8 September 1999

Abstract

Ions derived from electrospray ionization of poly(propylene imine) dendrimers (generations 1–5, synthesized from a 1,4-diaminobutane core) were subjected to ion trap tandem mass spectrometry. In some cases, ion/ion proton transfer reactions were used to form low charge state parent ions from higher charge state ions generated by electrospray. In addition, ion/ion proton transfer reactions performed on product ions formed by ion trap collisional activation of multiply charged parent ions facilitated interpretation of tandem mass spectrometry (MS/MS) spectra. Almost all of the products derived from dendrimer parent ions could be rationalized based on a set of dissociation processes involving a previously noted intramolecular nucleophilic attack by a nearest-neighbor nitrogen atom on a carbon alpha to a protonation site. For a given protonation site, attack can occur either from the adjacent nitrogen closer to the interior or closer to the exterior of the dendrimer. The processes that lead to the dominant products are highly dependent upon parent ion charge state. Singly charged ions fragment primarily by processes directed by protonation at a diaminobutane nitrogen whereas highly charged parent ions fragment largely by processes directed by protonation closer to the periphery of the dendrimer. MS/MS data for singly charged ions of series of synthesis failure products in the fourth and fifth generation dendrimers were collected. The results show that ion trap tandem mass spectrometry can provide information about the composition of mixtures of isomeric products resulting from side reactions that occur during the course of the multistep syntheses of the dendrimers. The data show, for example, that synthesis failures tend to occur on one side of the dendrimer. (Int J Mass Spectrom 195/196 (2000) 419–437) © 2000 Elsevier Science B.V.

Keywords: Poly(propylene imine) dendrimer; Quadrupole ion trap; Ion/ion proton transfer; Ion trap collisional activation

1. Introduction

The chemistry of gaseous macro-ions has become an active area of research with the advent of methods for forming such ions, such as matrix-assisted laser desorption ionization [1] and electrospray [2–5]. Ions derived from biopolymers, for example, have become the subjects of intense scrutiny. Attention has also been focused on ions derived from synthetic polymers [6–20]. The latter research has been devoted largely to linear synthetic polymers but there has been increasing attention devoted to hyperbranched polymers, such as dendrimers [21–29]. The latter species are of particular interest due to their relevance in the construction of well-defined three-dimensional structures from small molecular building blocks [30,31]. Just as it has been demonstrated that understanding the fragmentation behavior of ions derived from

* Corresponding author. E-mail: mcluckeysa@ornl.gov

Dedicated to the memory of Professor Robert R. Squires.

1387-3806/00/$20.00 © 2000 Elsevier Science B.V. All rights reserved

PII S1387-3806(00)00201-8

biopolymers can yield information regarding the primary structures of, e.g. a peptide or an oligonucleotide, understanding the ion chemistry of macro-ions derived from dendritic polymers might provide useful information about the structures of such polymers. Structural analysis tools for hyperbranched polymers based on MS/MS are likely to be useful in devising improved synthetic strategies.

Poly(propylene imine) dendrimers synthesized from a 1,4-diaminobutane (DAB) core are commercially available and are characterized by relatively simple chemical functionalities. They are comprised of tertiary nitrogens in the core of the polymer connected by saturated alkane chains. The two core nitrogens are separated by a four-carbon chain whereas the nitrogens in succeeding generations are separated by three-carbon chains. Error-free polymers contain tertiary nitrogens in the interior and primary nitrogens at the extremities of the chains. Electrospray ionization mass spectral data have been reported for poly(propylene imine) dendrimers along with mass spectrometry/mass spectrometry (MS/MS) data for selected charge states using triple quadrupole tandem mass spectrometry employing collisions with a gaseous target [32] and surface-induced dissociation (SID) [33]. These studies have indicated the major dissociation pathways of this class of dendrimer. The latter study, in particular, also addressed the role of parent ion charge state in determining the kinetic stability of the parent ion. It was noted that parent ion charge state was not a major factor in determining dendrimer ion stability, in contrast with some results obtained for polypeptide ions [34,35].

This study reports the behavior of positive ions of poly(propylene imine) dendrimers formed by electrospray ionization under ion trap collisional activation conditions. Particular emphasis was placed on the dissociation behavior of singly protonated ions for each generation of dendrimer. Electrospray ionization does not produce singly protonated ions for the higher generation dendrimers. Therefore, ion/ion proton transfer reactions [36,37] were used to convert highly charged ions formed by electrospray to singly protonated molecules prior to collisional activation. In some cases, collisional activation of multiply charged ions was followed by ion/ion reactions to convert product ions largely to singly charged ions [38] to verify the product ion charge states. Limited but useful structural information can be obtained from collisional activation of singly protonated ions. This information is most useful in drawing conclusions regarding the composition of isomeric mixtures resulting from side reactions that occur during the course of synthesis. This point is illustrated here with selected synthesis failure products observed in the fourth and fifth generation dendrimers.

2. Experimental

Poly(propylene imine) tetraamine dendrimers, generations 1–5, were purchased from Sigma (St. Louis, MO). In each case, the polymer was dissolved in a 75:25 methanol:water mixture to yield an approximate concentration of 25–50 μM. The solution was infused at a rate of 1.0 μL/min through a 100 μm inner diameter (i.d.) stainless steel capillary held at +3.5–4.0 kV.

All experiments were performed with a Finnigan ion trap mass spectrometer (ITMS™, San Jose, CA), modified for electrospray ionization. An electrospray interface/ion injection lens/ion trap assembly, which has been described previously [39], was mounted in a home-built vacuum system and connected with the electronics of the ITMS. When the experiments were repeated several months later, the interface had been modified by replacing the flat inlet aperture plate with a capillary inlet. The collisional activation data were essentially identical regardless of which interface design was used. In all cases, helium was introduced into the vacuum chamber, which was held at room temperature, to a total pressure (uncorrected) of 1.1×10^{-4} Torr, as measured with a Bayard-Alpert ionization gauge.

Following an ion accumulation period of 100–300 ms, dendrimer ions were isolated using either a single resonance ejection ramp or two resonance ejection ramps. In the former case, isolation of parent ions of interest having *m/z* values < 650 was effected using a single scan of the rf-voltage amplitude applied to the

ring electrode, which ejected lower mass ions by passing them through the $q_z = 0.908$ exclusion limit, whereas simultaneously applying a single frequency in dipolar fashion chosen to sweep out ions of *m/z* greater than that of the ion of interest. When the mass-to-charge ratio of the parent ion was greater than 650, the use of two resonance ejection ramps was necessary because the ejection of ions of *m/z* greater than 650 but less than that of the parent ion required a discrete resonance ejection step [40]. In the case of the $(M + H)^+$ ions derived from the fifth generation polymer, a wide *m/z* parent ion window was isolated that included many sequence failures of mass less than that of the complete polymer. In this case, particular parent ions were subjected to collisional activation as defined by the frequency and amplitude of the resonance excitation signal. MS^3 data were collected for a few of the major first generation product ions from the parent ions of the first two generation dendrimers. These experiments involved a subsequent ion isolation step after collisional activation of the initial parent ion to select the first generation product ion of interest, followed by collisional activation of the first generation product ion [41,42].

Conditions for ion trap collisional activation varied somewhat for the several dozen parent ions examined in this study. For all of the ions of generations 1–4, an activation time of 50 ms was used, whereas an activation time of 150 ms was used for the generation 5 ions. A longer activation time was used for the latter ions to increase the conversion of parent ions to product ions. The q_z values for the parent ions ranged from 0.078 for the $(M + H)^+$ ions of the fourth and fifth generation dendrimers (average masses 3513.9 and 7168.0, respectively) to as high as 0.207 for the $(M + H)^+$ ion of the first generation dendrimer (average mass = 316.5). The relative abundances of the product ions did not appear to be sensitive to the q_z value at which the parent ion was stored during activation. The resonance excitation amplitudes ranged from as low as 6 mV for the *m/z* 172 product ion from the first generation $(M + H)^+$ ion to as high as 500 mV for the singly protonated ions from the fifth generation polymer sample. It is possible to draw conclusions regarding ion stabilities by measuring ion trap collisional activation rates as a function of resonance excitation amplitude [43–46]. The measurement of relative ion stabilities, however, was not a focus of this study.

Ion/ion proton transfer reactions were used to form singly, doubly, and triply protonated parent ions from the parent ion charge state distributions of the fourth and fifth generation dendrimers. The procedure and instrumentation for effecting ion/ion proton transfer reactions in the quadrupole ion trap have been described [47]. In all cases, the positive dendrimer ions were injected into the ion trap first. Anions derived from glow discharge ionization of perfluoro-1,3-dimethylcyclohexane (PDCH) (Aldrich, Milwaukee, WI) were then injected into the ion trap for 20 ms and a mutual ion storage period of 50–100 ms was used to convert the highest charge state ions to lower charge states. The parent ion isolation step was then executed and followed by the collisional activation period. For the multiply charged parent ions, ion/ion proton transfer reactions were used to convert multiply charged product ions to singly charged product ions. In these cases, a 20 ms anion injection period and a mutual storage period of 100 ms was included *after* the parent ion isolation and collisional activation steps. These experiments were conducted to facilitate interpretation of the product ion spectra.

The normal mass-to-charge range of the ion trap was not extended for the ions derived from the first generation dendrimer. However, the *m/z* range of the ion trap was extended beyond the normal limit of 650 for all of the other experiments using resonance ejection [48]. All experiments involving the use of ion/ion reactions to reduce charge states employed a resonance ejection frequency of 29.45 kHz and an amplitude of 3 $V_{p\text{-}p}$. This set of conditions yielded an upper *m/z* limit of 7600. Data for the second generation ions (no ion/ion reactions) were collected using an *m/z* range extension factor of roughly 2 (resonance ejection frequency = 182.4 kHz, amplitude = 2.5 $V_{p\text{-}p}$). Data for the third and fourth generation dendrimers were collected using an *m/z* range extension factor of roughly 3 (119.7 kHz, 5.5 $V_{p\text{-}p}$). The mass spectral data and data for MS/MS of the $(M + 5H)^{5+}$ ion from the fifth generation dendrimer were collected

using an *m/z* range extension factor of roughly 4 (89.2 kHz, 5 $V_{p\text{-}p}$). MS/MS data for the $(M + 4H)^{4+}$ and $(M + 3H)^{3+}$ parent ions from the fifth generation dendrimer were acquired using 3 $V_{p\text{-}p}$ resonance ejection amplitudes and frequencies of 59.1 and 44.6 kHz, respectively. In all cases, the rate of change of the amplitude of the rf voltage applied to the ring electrode was the standard rate supplied by the ITMS electronics (128 V/ms). The *m/z* scales for the various MS/MS spectra were calibrated using the known average masses of the intact dendrimer ions. All spectra were acquired using the same voltages applied to the electron multiplier detector and conversion dynode. The MS/MS spectra were typically the average of 200–400 scans.

3. Results and discussion

The first generation dendrimer studied here was synthesized by Michael addition of four acrylonitrile molecules to 1,4-diaminobutane followed by hydrogenation of the cyano groups. Successive generations were constructed by alternating Michael addition and hydrogenation steps. The various generations have been denoted DAB-*dendr*-$(NH_2)_y$ where *Y* indicates the number of primary amines at the termini of the polymer [25]. For generations 1–5, $Y = 4$, 8, 16, 32, and 64, respectively. Generations 1 and 5 of DAB-*dendr*-$(NH_2)_y$ are indicated in Scheme 1. Results and discussion for data acquired for each of the generations are included in the following. Results are presented for the collisional activation of selected sequence failure products present in the fourth and fifth generations.

3.1. Generation 1, DAB-dendr-$(NH_2)_4$

Electrospray of the first generation polymer yielded the protonated molecule, $(M + H)^+$, almost exclusively under moderately gentle vacuum/atmosphere interface conditions. As the voltage gradients in the interface were increased, however, significant signals at *m/z* 186 and *m/z* 129 became apparent. These ions were also the major products observed

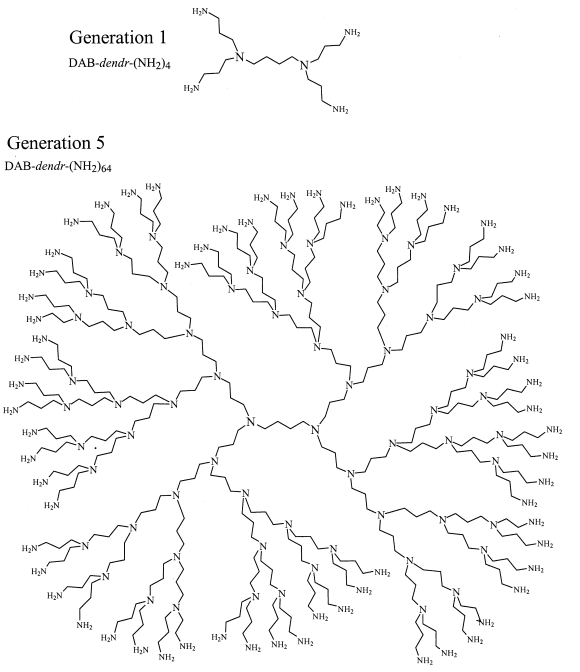

Scheme 1.

from ion trap collisional activation of the $(M + H)^+$ ion, as reflected in the MS/MS spectrum of Fig. 1(a). MS^n data were also collected whereby the *m/z* 186 product ($n = 3$) and the *m/z* 129 product ($n = 4$) were each isolated and subjected to collisional activation in turn. The results of these experiments are shown in Fig. 1(b) and (c), respectively. Scheme 2 summarizes the products formed from the $(M + H)^+$ ion as a result of the MS^3 experiments. Dashed lines in Scheme 2 indicate minor processes. The *m/z* 129 product is formed via the *m/z* 186 product as shown by the experiment leading to Fig. 1(b). It is likely that the *m/z* 129 ion in the MS/MS spectrum is formed via this sequence as well because it is difficult to draw a reasonable mechanism that would yield the *m/z* 129 product from a single step. Likewise, some of the products observed in the MS^3 experiment involving the *m/z* 186 product (viz, the *m/z* 112, *m/z* 84, and *m/z* 72 ions) are probably formed via further fragmentation of the *m/z* 129 ion.

The process where the *m/z* 186 ion is formed is a particularly important one for all of the dendrimers of

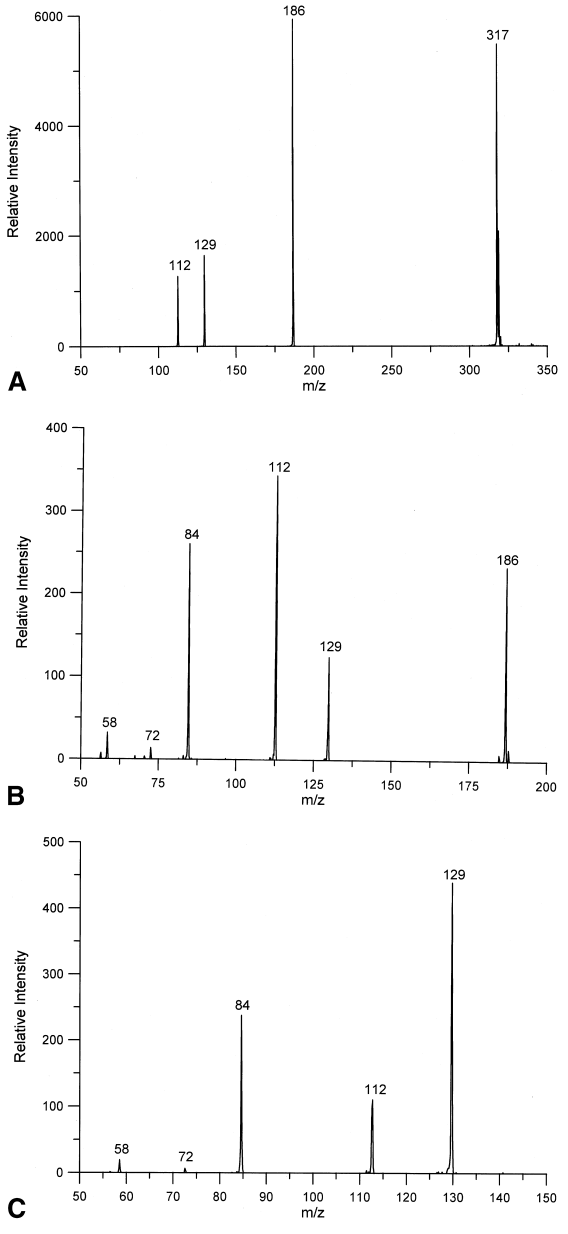

Fig. 1. (a) Ion trap MS/MS spectrum of the $(M + H)^+$ ion of DAB-*dendr*-$(NH_2)_4$ (generation 1, *m/z* 317). (b) MS^3 spectrum following the sequence *m/z* 317 → *m/z* 186 → products. (c) MS^4 spectrum following the sequence *m/z* 317 → *m/z* 186 → *m/z* 129 → products.

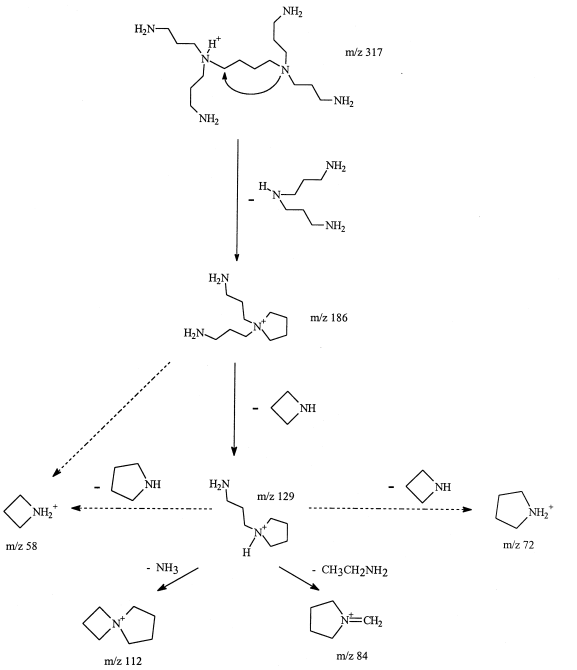

Scheme 2.

this kind. Both previous reports presenting decompositions of ions derived from poly(propylene imine) dendrimers described a rearrangement reaction leading to fragmentation whereby a carbon alpha to the protonated nitrogen is attacked by an adjacent nitrogen to yield a product ion with a quaternary nitrogen and an amine as a neutral product [32,33]. An arrow in Scheme 2 is shown indicating the attack of one of the DAB nitrogens (i.e. the generation 0 species) on the nearest alpha carbon, assuming protonation on the other DAB nitrogen. Such a generic mechanism was proposed earlier to describe fragmentations of protonated polytertiary amine hydrocarbons [49] and was referred to as an intramolecular nucleophilic substitution (S_Ni). The data reported here are consistent with S_Ni-type reactions being the major processes for decompositions of all of the dendrimers (see the following). In both the triple quadrupole collisional activation [32] and surface-induced dissociation [33] studies, nondissociative rearrangement reactions involving the S_Ni process were invoked to explain the appearance of some of the product ions. The rearrangements usually resulted from the attack on an alpha carbon adjacent to the charge site from a non-nearest nitrogen. Subsequent dissociation of the

rearranged ions could then lead to observed product ions directly from the usual S_Ni reaction. Such rearrangement reactions cannot be precluded from contributing to product ions observed in the MS^n studies described herein. However, the schemes shown here do not invoke rearrangement reactions of this sort. Rather, these schemes imply that the formation of some of the ions may proceed via decomposition mechanisms other than the S_Ni process. An example might be the loss of ethylamine from the *m/z* 129 product ion to yield the *m/z* 84 ion. In any case, data for the fourth and fifth generation dendrimers (see below) suggest that rearrangement reactions of the parent ions involving non-nearest neighbor nitrogens probably contribute very little to the ion trap MS/MS data.

3.2. Generation 2, DAB-dendr-$(NH_2)_8$

The electrospray mass spectra of the generation 2 dendrimer, DAB-*dendr*-$(NH_2)_8$, yielded the $(M + H)^+$ ion almost exclusively under the conditions used in this study. Fig. 2(a) displays the ion trap MS/MS spectrum of the parent ion and Fig. 2(b) and (c) show the results of the MS^3 experiments involving the *m/z* 414 and *m/z* 172 ions, respectively. Scheme 3 summarizes the product ions observed from the MS/MS and MS^3 experiments. [The formation of a product ion at *m/z* 58 may also occur under the conditions that led to Fig. 2(a) and (b) but the low *m/z* cutoff used during collisional activation precluded its storage.] The major product ions are consistent with S_Ni processes involving protonation of one of the DAB nitrogen atoms. The *m/z* 414 product is expected to arise from attack by the other DAB nitrogen atom via process A indicated in Scheme 3. The *m/z* 172 ion is expected to arise from attack by one of the two tertiary nitrogens added in the first generation step (process B in Scheme 3). The generation 2 ions are the first to illustrate a phenomenon that plays an important role in the appearance of the MS/MS spectra of the larger dendrimers. That phenomenon being, for a given site of protonation, the competition between S_Ni processes initiated by attack from nitrogens either closer to the core of the dendrimer or closer to the exterior.

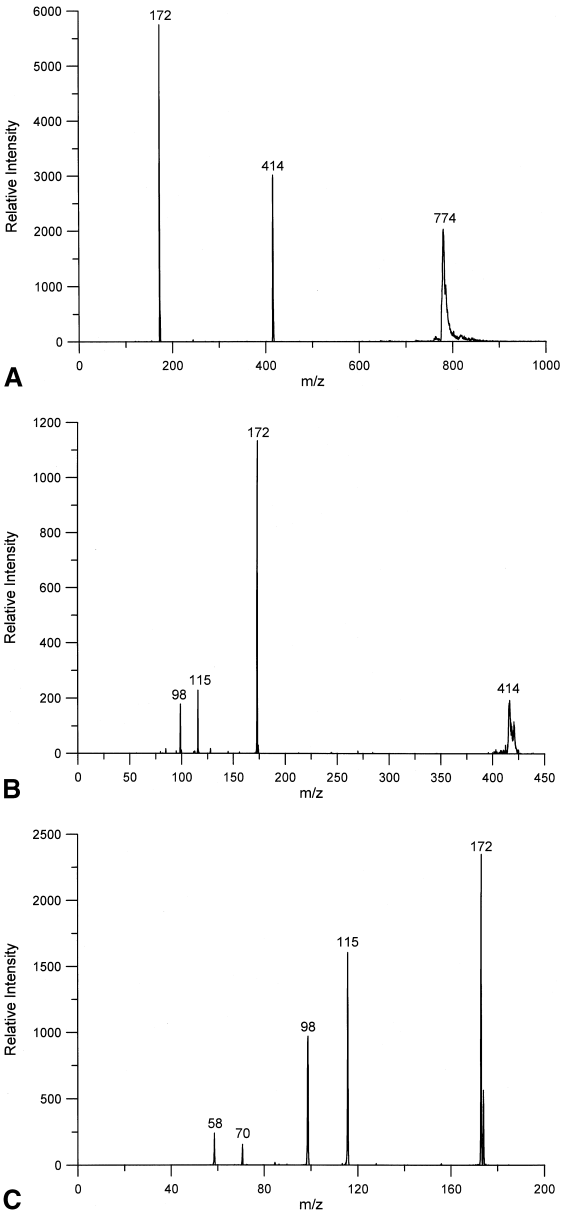

Fig. 2. (a) Ion trap MS/MS spectrum of the $(M + H)^+$ ion of DAB-*dendr*-$(NH_2)_8$ (generation 2, *m/z* 774). (b) MS^3 spectrum following the sequence *m/z* 774 → *m/z* 414 → products. (c) MS^3 spectrum following the sequence *m/z* 774 → *m/z* 172 → products.

3.3. Generation 3, DAB-dendr-$(NH_2)_{16}$

The third generation dendrimer is large and complex enough to make worthwhile the introduction of a

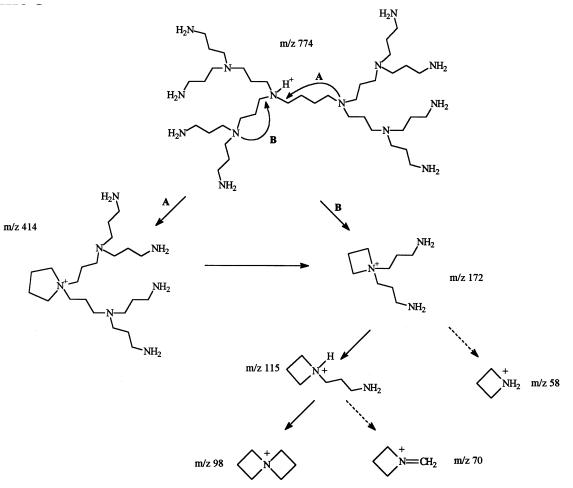

Scheme 3.

generalized scheme for labeling the various competitive decompositions that can contribute to the MS/MS spectrum. Such a scheme can be based on the possible S_Ni dissociations from protonation at the various generation tertiary nitrogens. These dissociations constitute well over 90% of those observed for all of the charge states of all dendrimers investigated. Scheme 4 shows the various dissociation channels as G_n(A) or G_n(B), where G_n represents the site of protonation, with $n = 0$ representing a DAB nitrogen (i.e. a nitrogen of the zero generation molecule), $n = 1$ representing the tertiary nitrogen introduced in the first generation, and so forth. Process A represents the S_Ni process involving attack on a carbon alpha to the charge site from the adjacent nitrogen in the interior of the polymer. Process B represents attack at a carbon alpha to the charge site from an adjacent nitrogen closer to the exterior of the polymer. Scheme 5 shows all of the possible G_n(A, B) products for the third generation $(M + H)^+$ ion along with their mass values. Virtually all of the products observed from the MS/MS spectra of the $(M + H)^+$ and $(M + 2H)^{2+}$ ions of DAB-*dendr*-$(NH_2)_{16}$ can be ascribed to one of these products. To make clear the origins of the major ions in the spectra, they are labeled according to the S_Ni process by which they likely originate [i.e. G_n(A or B)] and a subscript "*q*" or "*a*" is added to indicate that the product is the quaternary ammonium ion or the amine, respectively.

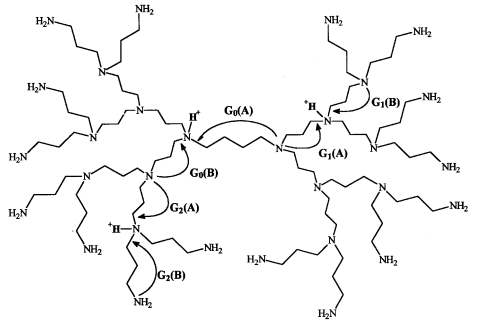

Scheme 4.

The electrospray mass spectrum of DAB-*dendr*-$(NH_2)_{16}$ showed both the singly and doubly protonated species. Fig. 3 shows the ion trap MS/MS spectrum of the $(M + H)^+$ ion with the product ions labeled according to Schemes 4 and 5. A wide parent ion isolation window was used in this case so that several of the synthesis failures gave rise to signals near that of the parent ion (i.e. all ions of *m/z* 1625 and greater). With the exception of the product ion at *m/z* 269, all of the products can be readily assigned as arising from S_Ni fragmentations directly from the parent ion. In all cases, the expected quaternary ammonium ions are formed. The G_0(A) and G_0(B) processes dominate suggesting protonation at one of the DAB nitrogens. A modest degree of proton transfer to tertiary nitrogens closer to the exterior is also suggested by the appearance of small signals that correspond to the quaternary ammonium ions expected from the G_1(A) and G_2(A) processes. The G_2(B) product could not be observed in this case because it fell below the low *m/z* cutoff used during collisional activation. An ion at *m/z* 172 is also observed, which corresponds to the expected G_1(B) product. However, it is also possible that at least some of the *m/z* 172 product ion could be formed from further dissociation of the larger first generation product ions. The *m/z* 269 ion, for example, must be formed from at least two dissociations and likely arises from loss of 131 Da [the mass of the amine formed in the G_2(A) process of Scheme 4] from the $G_0(B)_q$ product ion.

As discussed in the surface-induced dissociation

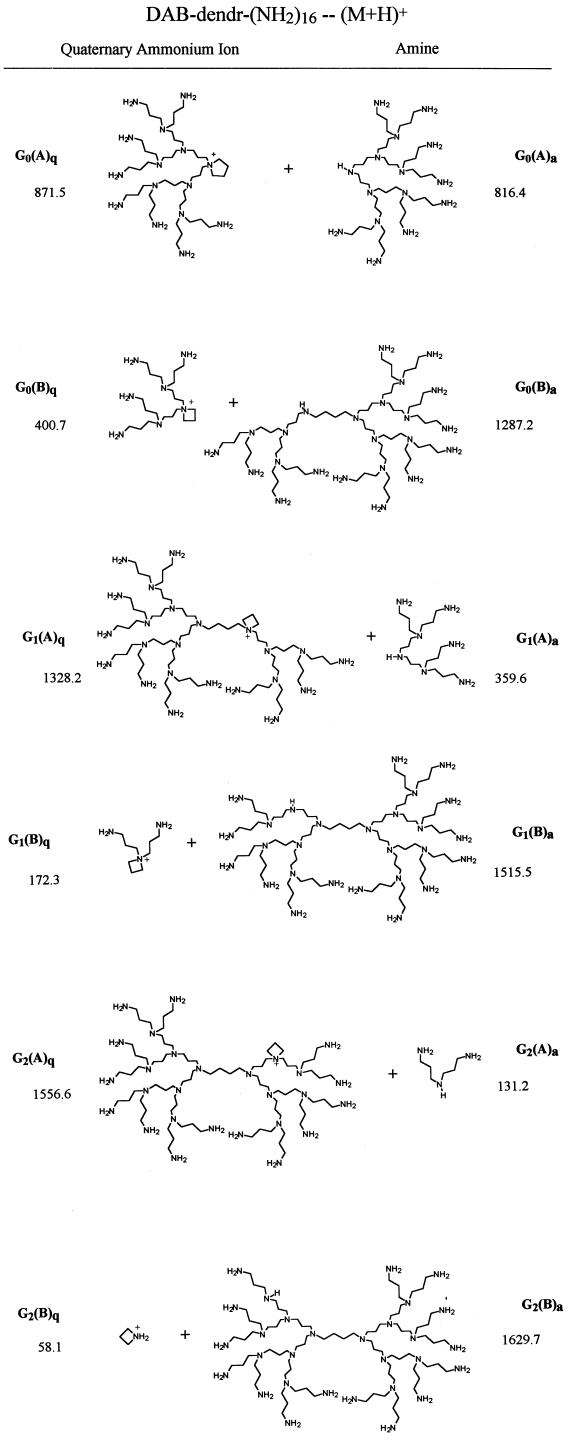

Scheme 5.

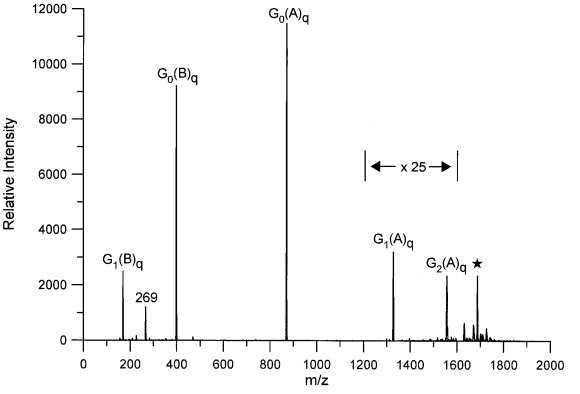

Fig. 3. Ion trap MS/MS spectrum of the $(M + H)^+$ ion of DAB-*dendr*-$(NH_2)_{16}$. The star indicates the *m/z* location of the parent ion.

study [33], multiple protonation of the dendrimer leads to Coulomb repulsion between charges which facilitates intramolecular proton transfer from intrinsically more basic sites to less basic ones if the relief of repulsion more than compensates for the difference in site basicities. Consistent with the SID results, the ion trap results also reflect a much larger contribution from dissociations directed by charge sites away from the DAB nitrogens. Fig. 4 provides exemplary data for the $(M + 2H)^{2+}$ ion of DAB-*dendr*-$(NH_2)_{16}$. Fig. 4(a) shows the conventional ion trap MS/MS spectrum and Fig. 4(b) shows the spectrum resulting from ion/ion proton transfer reactions involving the products in Fig. 4(a) and PDCH anions for 100 ms. The latter spectrum was used to facilitate interpretation of the conventional spectrum by removing product ion charge state ambiguities. [Ion/ion reaction data for product ion spectra were particularly useful for interpreting MS/MS spectra of the multiply charged fourth and fifth generation dendrimers (see the following).] In the case of the dissociation of a multiply protonated dendrimer, both products from a dissociation can carry a charge. Therefore, the amine product from the S_Ni process can appear as a product in the spectrum.

It is apparent from comparing the behavior of the $(M + H)^+$ ion with that of the $(M + 2H)^{2+}$ ion that far more fragmentation is directed by charge sites away from the core of the dendrimer in the case of the $(M + 2H)^{2+}$ ion. Although the G_0(A) and G_0(B)

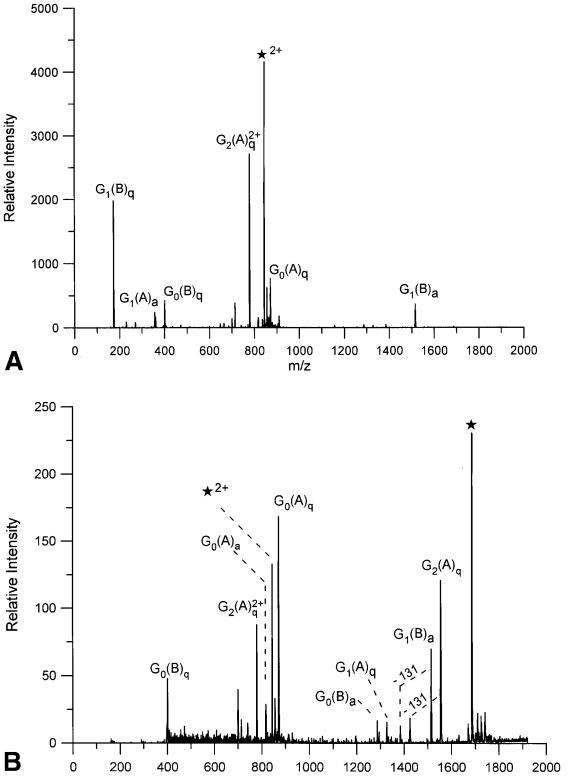

Fig. 4. (a) Ion trap MS/MS spectrum of the $(M + 2H)^{2+}$ ion of DAB-*dendr*-$(NH_2)_{16}$. The star indicates the *m/z* location of the $(M + 2H)^{2+}$ ion. (b) Post-ion/ion reaction spectrum of the product ions formed from collisional activation of the DAB-*dendr*-$(NH_2)_{16}$ $(M + 2H)^{2+}$ ion. The star indicates the *m/z* location of the $(M + H)^+$ ion.

processes make major contributions to the $(M + 2H)^{2+}$ data, there are also prominent signals arising from G_1(A), G_1(B), and G_2(A) processes. In fact, the loss of 131 Da, which corresponds to the G_2(A) process accounts for the largest product ion signal. Judging solely by the relative contributions of the various G_n processes, it would appear that most of the parent ions have charges on a G_1 nitrogen and on a G_2 nitrogen. However, it must also be recognized that there are more available channels for loss of 131 Da than for either the G_0 or G_1 processes.

3.4. Generation 4, DAB-dendr-$(NH_2)_{32}$

The competition between the A and B processes associated with the S_Ni mechanism for a given site of

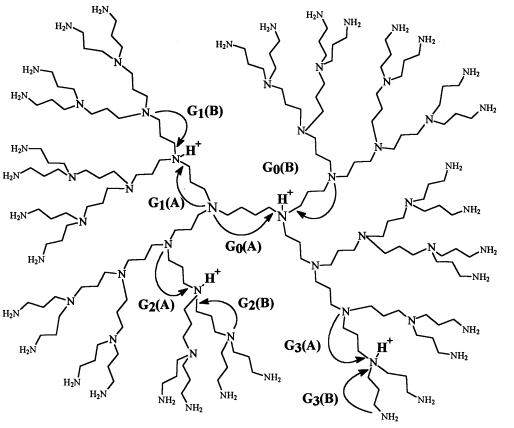

Scheme 6.

protonation and the importance of site(s) of protonation in determining the product ion spectra for the various charge states of a dendrimer are well illustrated with the fourth generation dendrimer. Scheme 6 indicates the various G_n S_Ni processes for DAB-*dendr*-$(NH_2)_{32}$ and Table 1 summarizes the expected masses of the quaternary ammonium ion and amine products from each S_Ni process from the $(M + H)^+$ ion. Fig. 5 shows electrospray mass spectra of DAB-*dendr*-$(NH_2)_{32}$ acquired both after ion/ion proton transfer reactions to convert most of the ions to $(M + H)^+$ species and before ion/ion reactions (inset of Fig. 5). The $(M + 3H)^{3+}$ ion is the base peak in the normal electrospray spectrum with lesser signals corresponding to the $(M + 4H)^{4+}$ and $(M + 2H)^{2+}$ ions. No signals corresponding to $(M + H)^+$ ions

Table 1
Masses (Da) of the quaternary ammonium ion and amine products from the various S_Ni processes of DAB-*dendr*-$(NH_2)_{32}$ $(M + H)^+$

S_Ni process	Quaternary ammonium ion	Amine
G_0(A)	1785	1729.9
G_0(B)	857.4	2657.5
G_1(A)	2698.5	816.4
G_1(B)	400.7	3114.2
G_2(A)	3155.3	359.6
G_2(B)	172.3	3342.6
G_3(A)	3383.7	131.2
G_3(B)	58.1	3456.8

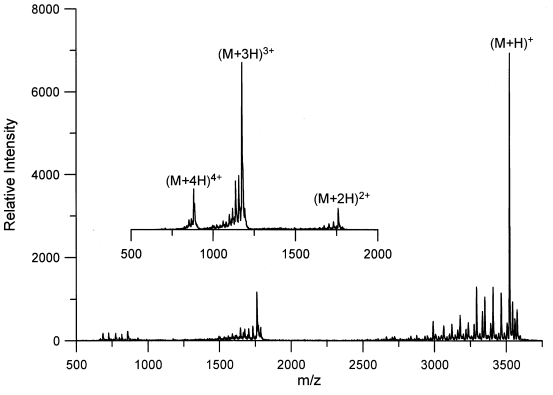

Fig. 5. Post ion/ion reaction electrospray (ES) mass spectrum of DAB-*dendr*-$(NH_2)_{32}$. The pre-ion/ion reaction electrospray mass spectrum of DAB-*dendr*-$(NH_2)_{32}$ (i.e. the normal ES mass spectrum) is shown in the inset.

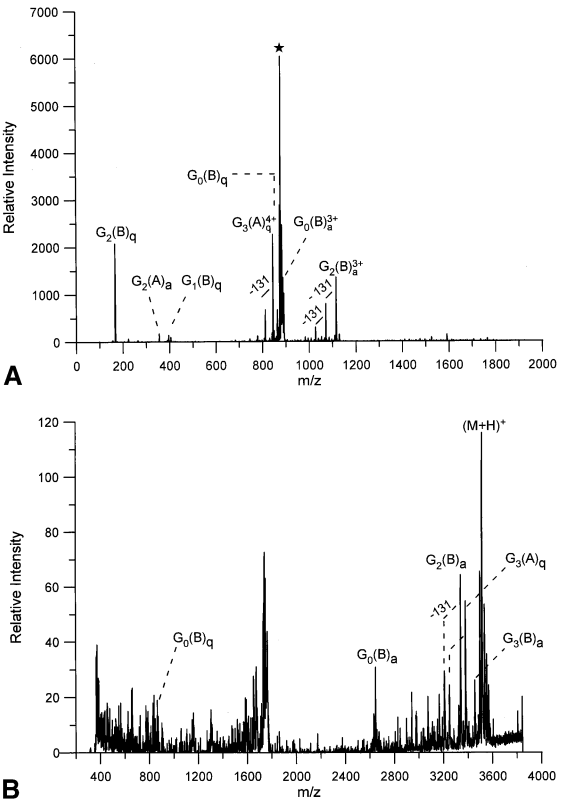

Fig. 6. (a) Ion trap MS/MS spectrum of the $(M + 4H)^{4+}$ ion of DAB-*dendr*-$(NH_2)_{32}$ (low *m/z* cutoff = 100). The star indicates the *m/z* location of the parent ion. (b) Post-ion/ion reaction spectrum of the product ions formed from collisional activation of the DAB-*dendr*-$(NH_2)_{32}$ $(M + 4H)^{4+}$ ion.

were observed to be formed directly by electrospray. The signals at lower *m/z* values than the $(M + nH)^{n+}$ signals at each charge state arise from side reactions during the course of polymerization that result in structural deficiencies. The major side reactions have been described as either incomplete Michael addition, leading to a mass deficiency of 57.1 Da, or ring formation during dehydrogenation, leading to a mass deficiency of 17.0 Da [25,32]. Multiple peaks arising from combinations of these side reactions can occur either in one step or can arise from the propagation of a synthesis failure in successive generations. Selected ions from the mixture of sequence failure species have been subjected to MS/MS and are discussed following presentation of the MS/MS data for multiply charged DAB-*dendr*-$(NH_2)_{32}$ ions.

Figs. 6–8 show the ion trap MS/MS spectra of the $(M + 4H)^{4+}$, $(M + 3H)^{3+}$, and $(M + 2H)^{2+}$ ions of DAB-*dendr*-$(NH_2)_{32}$, respectively, along with the post-ion/ion reaction data acquired for each charge state. The latter spectra were used in combination with the conventional MS/MS spectra to assign major product ions. In the case of the $(M + 4H)^{4+}$ ion, it is clear that two major S_Ni processes dominate. These are the G_2(B) (loss of the *m/z* 172 ion) and G_3(A) (loss of the 131 Da amine) processes, with the latter being slightly more prominent. Major signals also arise from apparent consecutive dissociations involving the loss(es) of the 131 Da amine. Signals that can be attributed to the G_3(B) amine, the G_0(B) quaternary ion and amine, and the G_1(B) quaternary ion were also identified in either the normal MS/MS spectrum or the post-ion/ion reaction spectrum. (Note that no product ions of *m/z* less than about 400 were recorded in the post-ion/ion reaction data because an anion ejection ramp was performed after the reaction period to remove the negative ions prior to mass analysis. This ramp also ejected positive ions of corresponding *m/z* values.)

The dissociation behavior of the triply protonated ion (Fig. 7) is also dominated by fragmentation arising from the second and third generation tertiary nitrogens. As with the quadruply protonated ion, loss

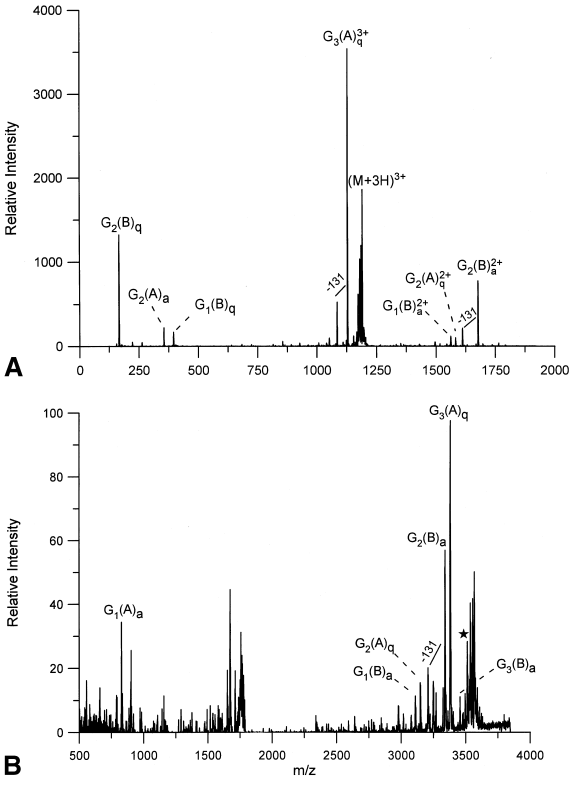

Fig. 7. (a) Ion trap MS/MS spectrum of the $(M + 3H)^{3+}$ ion of DAB-*dendr*-$(NH_2)_{32}$ (low *m/z* cutoff = 150). (b) Post-ion/ion reaction spectrum of the product ions formed from collisional activation of the DAB-*dendr*-$(NH_2)_{32}$ $(M + 3H)^{3+}$ ion. The star indicates the *m/z* location of the $(M + H)^+$ ion.

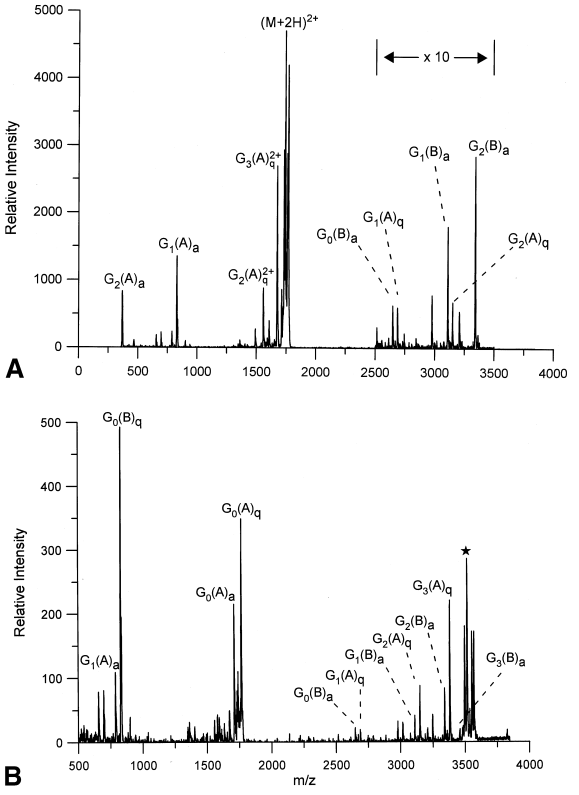

Fig. 8. (a) Ion trap MS/MS spectrum of the $(M + 2H)^{2+}$ ion of DAB-*dendr*-$(NH_2)_{32}$ (low *m/z* cutoff = 200). (b) Post-ion/ion reaction spectrum of the product ions formed from collisional activation of the DAB-*dendr*-$(NH_2)_{32}$ $(M + 2H)^{2+}$ ion. The star indicates the *m/z* location of the $(M + H)^+$ ion.

of the 131 Da amine, arising from the G_3(A) process, gives the most abundant product. Consecutive loss of two 131 Da amines is also observed as is loss of 131 Da from the G_2(B) amine product. Very little signal can be attributed to fragmentation arising from protonation at the DAB nitrogens.

Of all of the charge states of DAB-*dendr*-$(NH_2)_{32}$, the doubly protonated ion (Fig. 8) shows the most balanced contribution from fragmentation arising from all generations of tertiary nitrogens. In this case, the major signals arise from the G_0 processes. However, there are also clearly identifiable signals that can be attributed to all of the other major G_n processes. This result suggests that the presence of two charges in the DAB-*dendr*-$(NH_2)_{32}$ dendrimer combined with the internal energies accessed by the ion trap collisional activation process yields the greatest diversity in protonation sites. Such a conclusion, however, must be made with the proviso that the stabilities of the ions do not change significantly with charge state, as supported by the SID study [33].

As with the $(M + H)^+$ ions of all of the smaller dendrimers, almost all of the fragmentation of the singly protonated fourth generation dendrimer can be accounted for by the processes initiated by protonation at the DAB nitrogens (i.e. the G_0 processes) as indicated in Fig. 9(a). By far, the largest fragments correspond to the G_0(A) quaternary ammonium ion, which represents a splitting off of roughly half of the dendrimer, and the G_0(B) quaternary ammonium ion, which represents a splitting off of roughly three quarters of the dendrimer. Small signals are also

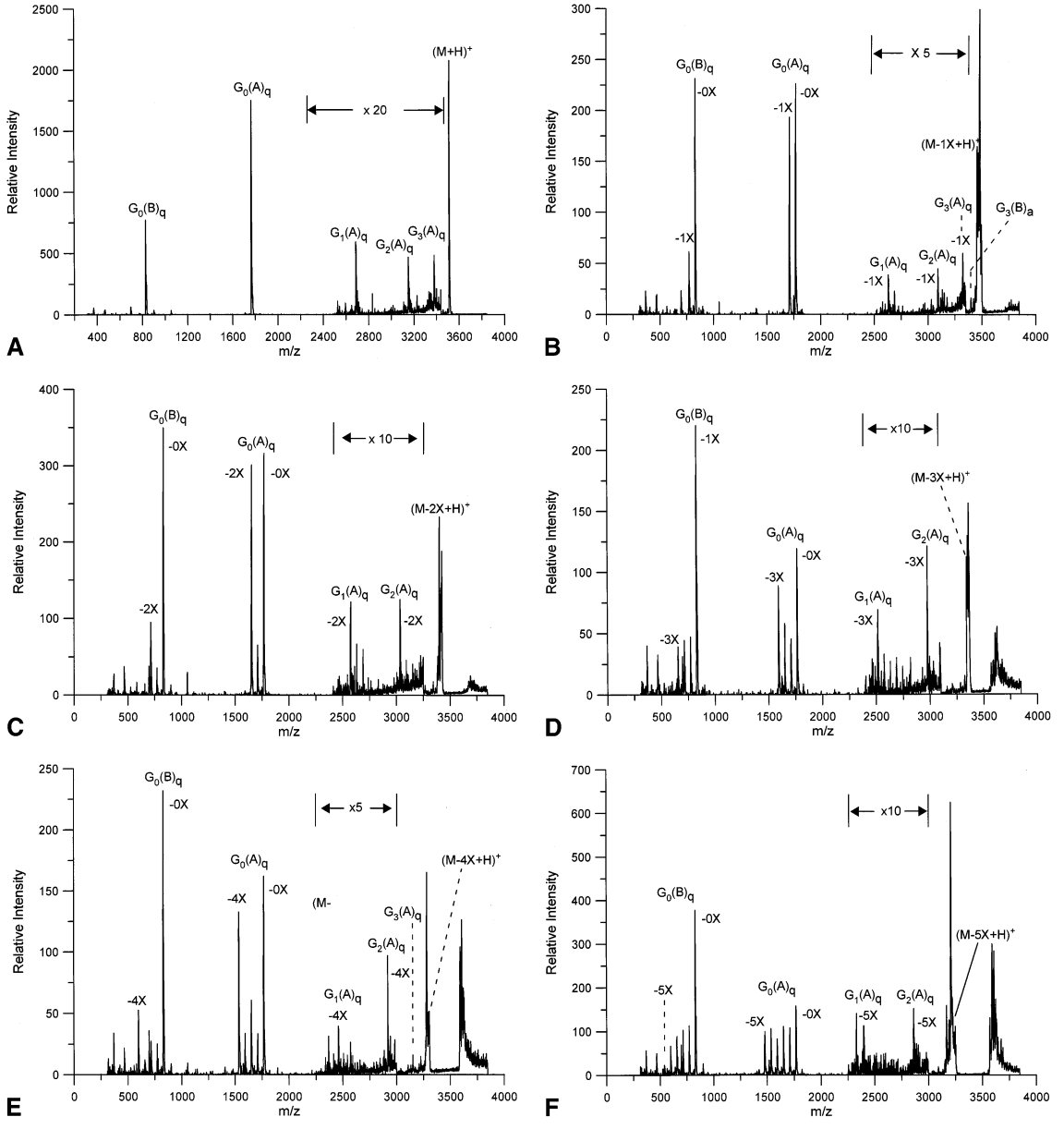

Fig. 9. (a) Ion trap MS/MS spectrum of the $(M + H)^+$ ion of DAB-*dendr*-$(NH_2)_{32}$ formed via ion/ion proton transfer reactions (low *m/z* cutoff = 300). The star indicates the *m/z* location of the $(M + H)^+$ ion. (b)–(f) MS/MS spectra of the incomplete synthesis products exhibiting mass deficiencies relative to that of the intact parent ion of *nX*, where $X = 57.1$ Da and $n = 1$–5.

observed for the G_1(A), G_2(A), and G_3(A) quaternary ammonium ions that correspond to the loss of roughly one-quarter, one-eighth, and one-sixteenth of the dendrimer, respectively.

We interrogated several of the singly protonated species that resulted following one or more failed Michael additions to determine what might be learned about the compositions of the mixtures likely to be present in the deficient dendrimers produced in the course of the multi-step synthesis. The MS/MS spec-

tra of the $(M - nX + H)^+$ ions, where X is 57.1 Da and $n = 1–5$, are shown in Fig. 9(b)–(f). The MS/MS spectrum of the $(M - X + H)^+$ ion is informative in terms of the relative propensities for loss of fragments containing the synthesis deficiency versus loss of fragments that do not. For example the $G_0(A)$ process, which splits the dendrimer into two nearly equal halves, would be expected to lead to two products of equal intensity in the MS/MS spectrum with one being deficient in mass by 57.1 Da, provided there is no preference for the formation of one product over the other. This is roughly seen to be the case [Fig. 9(b)]. For every n value of X there are $n + 1$ possible $G_0(A)$ products that can arise from all possible combinations of X deficiencies between the two halves of the dendrimer. The possibilities are bounded by the fragment with no X deficiencies and that with the maximum number of X deficiencies. These two fragments are related and should be of equal intensity provided there is no preference in dissociation to give one over the other. In general, fragments with mX deficiencies and $(n - m)X$ deficiencies are related and should appear in equal abundance. As seen in the spectra of Figs. 9(b)–(f), rough symmetry in the abundances of *related* ions is observed. However, the total abundances of related pairs of ions relative to one another is governed by the composition of the isomeric mixture that comprises the parent ion population.

If it is assumed that there is no significant two-step fragmentation, or, if so, that it depletes all of the $G_0(A)_q$ ions equally, the products from the $G_0(A)$ process provide direct, albeit limited, information about the composition of the mixture of structures present in the $(M - nX + H)^+$ ion populations for $n > 1$. For example, Fig. 9(c), which shows the MS/MS spectrum of the $(M - 2X + H)^+$ ions, indicates that roughly 90% of the species in the parent ion mixture experienced failed Michael additions on the same half of the dendrimer, which differs significantly from the statistical expectation for random independent failures. Similarly, all of the $(M - nX + H)^+$ ions for $n > 1$ show $G_0(A)_q$ product ion relative abundances that differ significantly from statistical expectation for random Michael addition failures in the last step of the synthesis. Of course, the actual mixture composition is affected by events that occur in each of the steps of the synthesis. For all of the $(M - nX + H)^+$ ions studied here, with the exception of the $(M - 5X + H)^+$ ion, there is a strong tendency for all of the mass deficit to be present on one side of the dendrimer.

The $G_0(B)$ process leads to the formation of an ion that represents roughly one quarter of the original dendrimer parent ion. In this case, for the $(M - X + H)^+$ ion, one-fourth of the $G_0(B($$_q$ ions would be expected to show the X deficit. In Fig. 9(b), roughly 21% of the $G_0(B)_q$ ions show the X deficit. Based on the limited ion statistics associated with this experiment, it cannot be concluded that there is a significant preference for formation of $G_0(B)_q$ ions without an X deficit. In any case, the data for the other $(M - nX + H)^+$ ions strongly suggest that at least qualitative information can be obtained from the relative abundances of the $G_0(B)_q$ ions. For example, the $G_0(B)_q$ ions formed from the $(M - 2X + H)^+$ parent [Fig. 9(c)] show the fragment missing $2X$ to be over twice the abundance of the product missing X. This observation suggests that most of the failed Michael additions took place on the same quarter of the dendrimer, and is consistent with the implication of the abundances of the $G_0(A)_q$ ions that both Michael additions took place on the same half of the dendrimer roughly 90% of the time. Similarly, the data for the $(M - 4X + H)^+$ ion [Fig. 9(e)] suggest that the major mixture component was comprised of species in which all of the mass deficit ($4X$) was present on the same quarter of the dendrimer.

The other processes observed to occur [viz. the $G_1(A)$, $G_2(A)$, and $G_3(A)$ processes], can also, in principle, yield information about the composition of the mixtures of synthesis failure products. The $G_1(A)$ process should give information complementary to that provided by the $G_0(B)$ process and the $G_2(A)$ and $G_3(A)$ processes should provide information about the distribution of sequence failures at the levels of one-eighth and one-sixteenth of the dendrimer. However, these processes are minor ones and the ion statistics associated with their products are limited. Perhaps the doubly protonated ion, which shows

Table 2
Masses (Da) of the quaternary ammonium ion and amine products from the various S_Ni processes of DAB-*dendr*-$(NH_2)_{64}$ $(M + H)^+$

S_Ni process	Quaternary ammonium ion	Amine
G_0(A)	3612.1	3557.0
G_0(B)	1771.0	5398.0
G_1(A)	5439.1	1729.9
G_1(B)	857.4	6311.6
G_2(A)	6352.6	816.4
G_2(B)	400.7	6768.3
G_3(A)	6809.4	359.6
G_3(B)	172.3	6996.7
G_4(A)	7037.8	131.2
G_4(B)	58.1	7110.9

larger contributions for the G_1, G_2, and G_3 processes than does the $(M + H)^+$ ion, could provide this information. Furthermore, MS^n experiments involving the $G_0(A)_q$ and $G_0(B)_q$ ions might also be expected to yield further information. No such experiments were conducted in this study but it is clear from the data of Fig. 9 that at least limited composition information can be obtained via MS/MS of the various synthesis failure mixtures.

3.5. Generation 5, DAB-dendr-$(NH_2)_{64}$

The electrospray mass spectrum of the DAB-*dendr*-$(NH_2)_{64}$ dendrimer showed large signals for the $(M + 5H)^{5+}$ and $(M + 4H)^{4+}$ species. MS/MS data were collected for the +1–+5 charge states whereby ion/ion reactions were used to form the +1–+3 charge states from the +5 and +4 charge states. Table 2 lists the masses of both the quaternary ammonium ion and amine products that are expected to be formed from the various major S_Ni processes. As with the other multiply charged dendrimer parent ions, ion/ion proton transfer reactions were also conducted to facilitate interpretation of the MS/MS data. Many of the observations already noted for the fourth generation dendrimer were also noted for the fifth generation dendrimer. Therefore, only a limited data set is presented here.

Fig. 10 shows the MS/MS spectrum of the $(M + 4H)^{4+}$ parent ion. The assignments shown in the

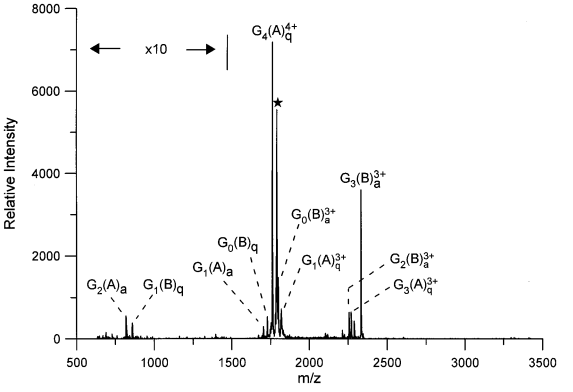

Fig. 10. Ion trap MS/MS spectrum of the $(M + 4H)^{4+}$ ion of DAB-*dendr*-$(NH_2)_{64}$ (low *m/z* cutoff = 600). The star indicates the *m/z* location of the $(M + 4H)^{4+}$ ion.

spectrum were derived in part from interpretation of the post-ion/ion reaction spectrum (not shown). As with the higher charge states of the fourth generation ion, by far the major processes observed in this case correspond to those initiated by protonation sites near the exterior of the dendrimer. Specifically, they were the loss of the 131 Da amine [process G_4(A)] and the loss of the *m/z* 172 quaternary ammonium ion [process G_3(B)]. Small signals were also observed for the G_0(B), G_1(A), G_1(B), G_2(A), G_2(B), and G_3(A) processes.

Also in analogy with the fourth generation dendrimer, the $(M + 2H)^{2+}$ ion of DAB-*dendr*-$(NH_2)_{64}$ shows a fragmentation pattern that most evenly represented the various S_Ni processes. Fig. 11 shows, in this case, the post-ion/ion reaction spectrum of the product ions formed via ion trap collisional activation of the $(M + 2H)^{2+}$. Product ions can be identified that result from each of the major S_Ni processes. Interestingly, the major products arise from the G_0 processes and the G_4 processes. This observation is consistent with protonation sites at a DAB nitrogen (generation 0) and at a generation 4 tertiary nitrogen. However, significant abundances of products from G_1–G_3 processes suggests a fairly high degree of proton mobility in the activated $(M + 2H)^{2+}$ ions or a parent ion population with protonation sites already distributed throughout the dendrimer.

MS/MS data were also collected for $(M - nX +$

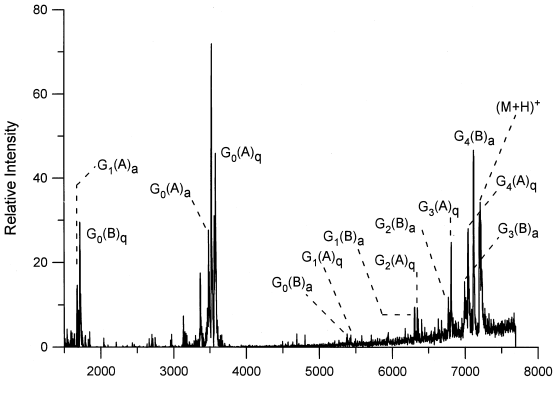

Fig. 11. Post-ion/ion reaction spectrum of the product ions formed from collisional activation of the DAB-*dendr*-$(NH_2)_{64}$ $(M + 2H)^{2+}$ ion (low *m/z* cutoff = 600).

$H)^+$ ions, where *n* in this case was 0–8. All parent ions were formed from the higher charge states by ion/ion proton transfer reactions. Fig. 12(a) shows a spectrum of the +1 charge region of DAB-*dendr*-$(NH_2)_{64}$ after an ion/ion proton transfer reaction period of about 100 ms. The pattern of relative abundances of the sequence failure products matches closely the charge-state deconvoluted data reported by Hummelen et al. for this dendrimer [25] and the predicted abundance distribution based on a statistical simulation of the data described by these authors. Fig. 12(b) shows the MS/MS spectrum of the $(M + H)^+$ ion. In analogy with the other singly protonated dendrimers, the dominant dissociation products arise from the G_0(A) and G_0(B) processes. This observation is consistent with protonation of a core nitrogen. Small signals are also observed for the quaternary ammonium ion products from the G_1(A) and G_2(A) processes. A wide parent ion isolation window was used to collect the $(M - nX + H)^+$ data which precluded the observation of the quaternary ammonium products from the G_3(A) and G_4(A) processes. Based on the MS/MS behavior of other $(M + H)^+$ ions, these products might be expected to be present, but at abundances comparable to or lower than those of the G_1(A) and G_2(A) processes. The region of the isolated band of parent ions that was subjected to collisional activation is clearly apparent in Fig. 12(b) from the significant diminution in parent ion signal at and around *m/z* 7169.

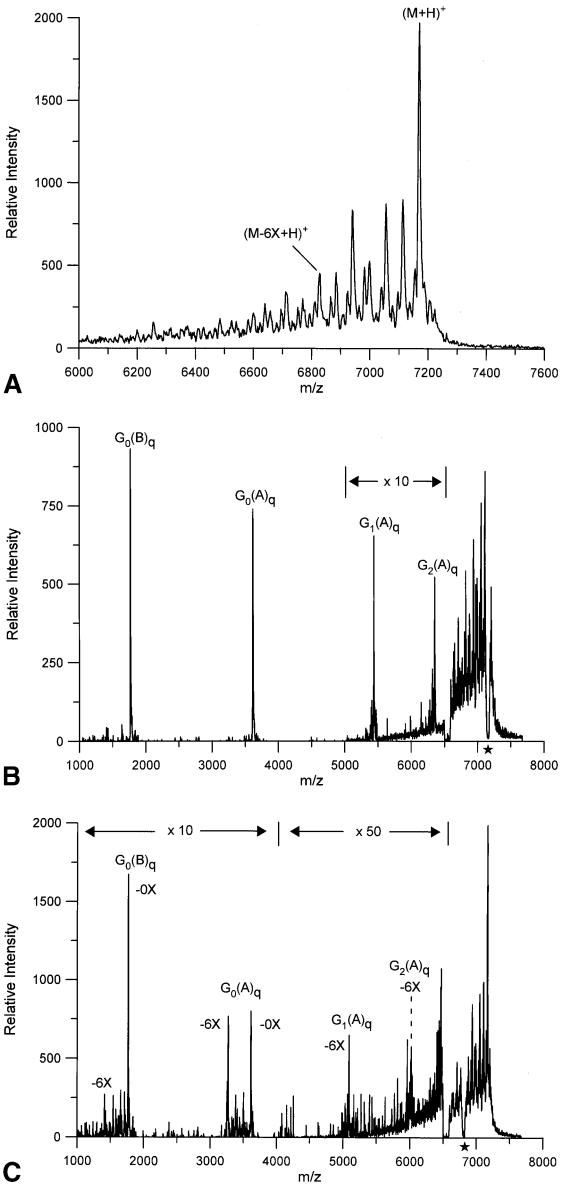

Fig. 12. (a) Expanded view of the $(M + H)^+$ *m/z* region on an electrospray mass spectrum of a freshly prepared solution of DAB-*dendr*-$(NH_2)_{64}$. The $(M + H)^+$ ions were formed from higher charge states via ion/ion proton transfer reactions. (b) MS/MS spectrum of the $(M + H)^+$ ion of DAB-*dendr*-$(NH_2)_{64}$ (low *m/z* cutoff = 600). A wide parent ion isolation window was employed. A much narrower window of ions were activated, however, as determined by the frequency and amplitude of the resonance excitation signal. The star indicates the *m/z* location of the $(M + H)^+$ ion. (c) MS/MS of the $(M - 6X + H)^+$ ion, where $X = 57.1$ Da.

The same qualitative behavior noted for the dissociation of the $(M - nX + H)^+$ ions of DAB-*dendr*-$(NH_2)_{32}$ was observed for the $(M - nX + H)^+$ ions of DAB-*dendr*-$(NH_2)_{64}$. Of particular note was the observation that most of the sequence failures tended to be on one side of the dendrimer for all of the $(M - nX + H)^+$ ions studied. An example is given in Fig. 12(c), which shows the MS/MS spectrum of the $(M - 6X + H)^+$ ion. As with the G_0(A) products from all of the $(M - nX + H)^+$ products, rough symmetry in ion abundances is observed for the related G_0(A) quaternary ammonium ions from the $(M - 6X + H)^+$ ion (i.e. products with mass deficiencies of $X = 0,6$, 1,5, 2,4, and 3,3 are related). Clearly, most of the $(M - 6X + H)^+$ isomers resulted from failed Michael additions on one side of the dendrimer. The next most abundant major class of isomers showed four failed Michael additions on one side of the dendrimer and two on the other. Relatively small fractions of the isomeric mixture were comprised of isomers with three Michael addition failures on each side of the dendrimer and isomers with one and five failed Michael additions, respectively, on each side. The G_0(B) product abundances are consistent with the information suggested by the abundances of the G_0(A) products. For example the quaternary ammonium G_0(B) products with five and three failed Michael additions are low in abundance relative to those with one, two, four, or six failed Michael additions. Such an observation might be expected based on the knowledge that there are relatively few isomers with five or three failed Michael additions on a side. Note also that the G_0(B) products suggest that a significant fraction of the parent ion population arose from six failed Michael additions on one quarter of the dendrimer. The high abundance of the G_0(B) product with no missing Michael additions is also consistent with the tendency for synthesis failures to be concentrated on one side of the dendrimer.

It was noted during the course of this study that solutions allowed to stand for lengthy periods of time showed measurable changes in the electrospray mass spectra. Data collected from an aged solution (15 weeks at room temperature in the laboratory) are shown here to illustrate the utility of tandem mass

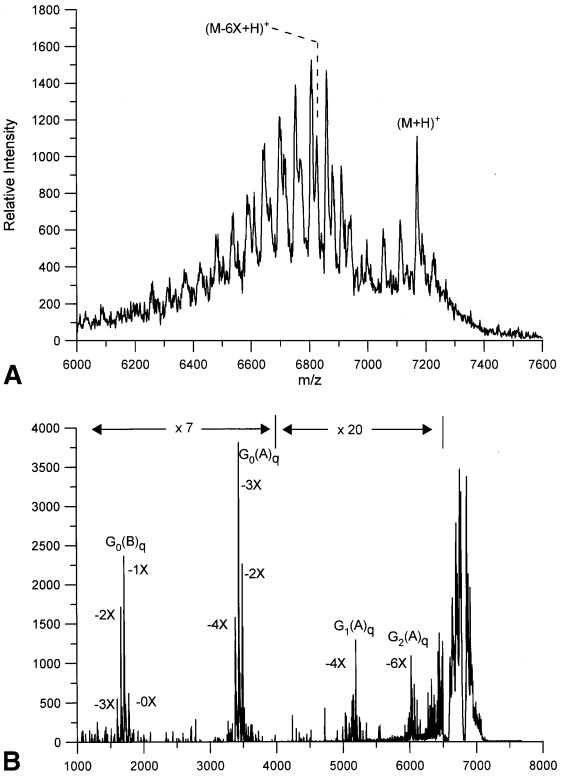

Fig. 13. (a) Expanded view of the $(M + H)^+$ *m/z* region of the electrospray mass spectrum of an aged solution of DAB-*dendr*-$(NH_2)_{64}$. The solution was prepared in identical fashion to the solution leading to Fig. 12 but was subjected to storage at room temperature for fifteen weeks before data collection. The $(M + H)^+$ ions were formed from higher charge states via ion/ion proton transfer reactions. (b) MS/MS of the $(M - 6X + H)^+$ ion, where $X = 57.1$ Da.

spectrometry in studying the composition of dendrimer mixtures with synthesis failures. Fig. 13(a) shows the +1 region of the aged DAB-*dendr*-$(NH_2)_{64}$ solution whereby the +1 ions were formed by ion/ion reactions involving the higher charge states formed by electrospray. This spectrum can be compared directly with Fig. 12(a). Note the significant change in the abundance distribution of products. There is a significant diminution in the $(M + H)^+$ signal and an overall shift to lower mass products. It is also clear that the products that show at least one ammonia loss are far more prominent in the aged solution. Clearly, reactions occurred upon storage that resulted in the partial decomposition (and, perhaps, rearrangement

without a change in mass) of some of the dendrimers. Tandem mass spectrometry was performed on most of the same nominal $(M - nX + H)^+$ ions studied from freshly prepared solutions. Note that the mass spectra and MS/MS spectra of fresh solutions were highly reproducible over many months. Furthermore, the MS/MS spectra of the $(M - 0x + H)^+$ ions from fresh and aged solutions were identical (data not shown).

Fig. 13(b) shows the MS/MS spectrum obtained for the $(M - 6X + H)^+$ ion derived from the aged solution. This spectrum was acquired under conditions identical to those used to obtain the MS/MS data of Fig. 12(c). It is obvious from the comparison of Figs. 13(b) and 12(c) that the isomeric compositions of the mixtures comprising the $(M - 6X + H)^+$ ion populations of the fresh and aged solutions are markedly different. In stark contrast with the data for the fresh solution, the G_0(A) products show that the $(M - 6X + H)^+$ ions from the aged mixture are largely comprised of ions with an even distribution of mass defects. That is, there are roughly equal numbers of mixture components missing $3X$ on each side and missing $4X$ and $2X$ on the sides. Very little evidence for the $0X$:$6X$ combination, which was the dominant combination from the fresh solution, is present.

The aged solution shows a much more statistical distribution of mass decrement than does the fresh solution. Dramatic differences are also observed in the distributions of the G_0(B) products from the fresh and aged solutions. In sharp contrast with the results for the fresh solution, the aged solution shows G_0(B) products with one and two missing Michael additions per quadrant to be most abundant. Little or no signal arising from $G_0(B)_q$ ions missing four, five, or six Michael additions is observed. Furthermore, the signal due to the G_0(B) ion with no missing Michael additions is greatly diminished in the aged solution data relative to the fresh solution data. These observations collectively support the conclusion that the mixture composition of $(M - 6X + H)^+$ ions formed from the aged solution approximates a statistical distribution of missing C_3H_7N groups (i.e. the moiety of mass = X = 57.1 Da) far more closely than does the mixture composition of $(M - 6X + H)^+$ ions formed from the freshly prepared solution.

It is important to recognize that any significant degree of parent ion rearrangement that occurs as a result of the ion activation process can compromise the utility of MS/MS in providing valid information about the composition of isomeric mixtures of the dendrimers with missing pieces. An example of a plausible rearrangement is the attack by a non-nearest-neighbor nitrogen on a carbon alpha to a protonation site. Such a rearrangement can lead to a new parent ion structure. The results of this study cannot preclude categorically the involvement of rearrangement reactions that alter the original connectivity of the parent ion. However, if they were important for the dendrimer $(M + H)^+$ and $(M - nX + H)^+$ ions studied here, S_Ni decomposition reactions from the rearranged ions would be expected to yield product ions with masses other than those expected from the highly symmetric dendrimer. Contributions to the MS/MS spectra from unexpected or uninterpretable products were not noted, suggesting that parent ion rearrangement might give rise to misleading structural information does not occur under these ion activation conditions to a significant extent.

4. Conclusions

The poly(propylene imine) dendrimers show relatively simple decomposition chemistry under ion trap collisional activation conditions. The primary decomposition reactions are consistent with the general S_Ni mechanisms described previously for polytertiary amines [49] and for these dendrimers activated by other means [32,33]. Virtually all of the products in the MS/MS spectra can be interpreted on the basis of S_Ni reactions involving attack from a neutral nitrogen that is either interior to or exterior to the protonation site, where “interior” is defined as closer to (or one of) the nitrogen atoms of DAB. The possibility for protonation at tertiary nitrogens arising from each successive stage of synthesis gives rise to a suite of possible decomposition channels. The extent to which each of these channels contributes to the MS/MS

spectrum is highly dependent upon charge state. This charge state effect is most easily rationalized on the basis of changes in favored sites of protonation as a result of coulomb repulsion associated with multiple protonation. Highly charged ions tend to fragment nearer to the periphery of the dendrimer than do ions of low charge state. Singly protonated ions for all dendrimer generations show fragmentation that is consistent with protonation predominantly at a DAB nitrogen.

Ion trap tandem mass spectrometry promises to be a useful tool in drawing conclusions about the composition of isomeric mixtures arising from side reactions associated with dendrimer synthesis. Data for a solution allowed to age for several months at room temperature also suggest that tandem mass spectrometry can provide information about the changes in mixture compositions of dendrimers that undergo reactions in solution. The $(M + H)^+$ ions provide information about the distribution of synthesis failures at the one-half and one-quarter dendrimer levels via the G_0(A) and G_0(B) processes, respectively. Although multiply charged dendrimers with failed Michael addition products were not subjected to study, the MS/MS results for multiply charged intact dendrimers suggest that information at the one-eighth and higher levels might be accessible by ion trap MS/MS of multiply charged ions, due to the greater contributions to the product ion spectra from S_Ni processes that occur nearer to the periphery of the dendrimer.

Acknowledgements

Research sponsored by the Division of Chemical Sciences, Office of Basic Energy Sciences, U.S. Department of Energy, under contract no. DE-AC05-96OR22464 with Oak Ridge National Laboratory, managed by Lockheed Martin Energy Research Corp. One of the authors (T.G.S.) acknowledges support through appointments to the Oak Ridge National Laboratory Postdoctoral Research Associates Program administered jointly by the Oak Ridge Institute for Science and Education and Oak Ridge National Laboratory.

References

[1] M. Karas, F. Hillenkamp, Anal. Chem. 60 (1988) 2299.
[2] J.B. Fenn, M. Mann, C.K. Meng, S.F. Wong, C.M. Whitehouse, Science 246 (1989) 64.
[3] J.B. Fenn, M. Mann, C.K. Meng, S.F. Wong, C.M. Whitehouse, Mass Spectrom. Rev. 9 (1990) 37.
[4] R.D. Smith, J.A. Loo, C.G. Edmonds, C.J. Barinaga, H.R. Udseth, Anal. Chem. 62 (1990) 882.
[5] R.D. Smith, J.A. Loo, R.R. Ogorzalek Loo, M. Busman, H.R. Udseth, Mass Spectrom. Rev. 10 (1991) 359.
[6] G. Montaudo, Trends Polym. Sci. 4 (1996) 81.
[7] U. Bahr, A. Deppe, M. Karas, F. Hillenkamp, U. Giessmann, Anal. Chem. 62 (1992) 2866.
[8] P.O. Danis, D.E. Karr, D.G. Westmoreland, M.C. Piton, D.I. Christie, P.A. Clay, S.H. Kable, R.G. Gilbert, Macromolecules 26 (1993) 6684.
[9] P.O. Danis, D.E. Karr, Y. Xiong, K.G. Owens, Rapid Commun. Mass Spectrom. 10 (1996) 862.
[10] D.C. Schreimer, L. Li, Anal. Chem. 68 (1996) 2721.
[11] D.C. Schreimer, L. Li, Anal. Chem. 69 (1997) 4169.
[12] D.C. Schreimer, L. Li, Anal. Chem. 69 (1997) 4176.
[13] A.T. Jackson, H.T. Yates, J.H. Scrivens, M.R. Green, R.H. Bateman, J. Am. Soc. Mass Spectrom. 8 (1997) 1206.
[14] A.T. Jackson, H.T. Yates, J.H. Scrivens, G. Critchley, J. Brown, M.R. Green, R.H. Bateman, Rapid Commun. Mass Spectrom. 10 (1996) 1668.
[15] T. Wyttenbach, G. von Helden, M.T. Bowers, Int. J. Mass Spectrom. Ion Processes 165 (1977) 377.
[16] C.E.C.A. Hop, R.J. Bakhtiar, J. Chem. Ed. 73 (1996) A162.
[17] R. Saf, C. Mirtl, K. Hummel, Acta Polym. 48 (1997) 513.
[18] L. Prokai, W.J. Simonsick Jr., Rapid Commun. Mass Spectrom. 7 (1993) 853.
[19] M.W.F. Nielen, Rapid Commun. Mass Spectrom. 10 (1996) 1652.
[20] C.N. McEwen, W.J. Simonsick Jr., B.S. Larsen, K. Ute, Hatada, J. Am. Soc. Mass Spectrom. 6 (1995) 906.
[21] G.J. Kallos, D.A. Tomalia, D.M. Hedstrand, S. Lewis, J. Zhou, Rapid Commun. Mass Spectrom. 5 (1991) 383.
[22] L. Paša Tolić, G.A. Anderson, R.D. Smith, H.M. Brothers II, R. Spindler, D.A. Tomalia, Int. J. Mass Spectrom. Ion Processes 165/166 (1997) 405.
[23] B.L. Schwartz, A.L. Rockwood, R.D. Smith, D.A. Tomalia, R. Spindler, Rapid Commun. Mass Spectrom. 9 (1995) 1552.
[24] D. Stökigt, G. Lohmer, D. Belder, Rapid Commun. Mass Spectrom. 10 (1996) 521.
[25] J.C. Hummelen, J.L.J. van Dongen, E.W. Meijer, Chem. Eur. J. 3 (1997) 1489.
[26] Sj. van der Wal, Y. Mengerink, J.C. Brackman, E.M.M. de Brabander, C.M. Jeronimus-Stratingh, A.P. Bruins, J. Chromatogr. A 825 (1998) 135.
[27] J.W. Kriesel, S. König, M.A. Freitas, A.G. Marshall, J.A. Leary, T.D. Tilley, J. Am. Soc. Mass Spectrom. 120 (1998) 12207.
[28] J.K. Gooden, M.L. Gross, A. Mueller, A.D. Stefanescu, K.L. Wooley, J. Am. Chem. Soc. 120 (1998) 10180.
[29] L.J. Hobson, W.J. Feast, Polymer 40 (1990) 1279.

[30] D.A. Tomalia, A.M. Naylor, W.A. Goddard III, Angew. Chem., Int. Ed. Engl. 29 (1990) 138.
[31] J.M.J. Frechet, Science 263 (1994) 1710.
[32] J.W. Weener, J.L.J. van Dongen, J.C. Hummelen, E.W. Meijer, Polym. Mater. Sci. Eng. 77 (1997) 147.
[33] J. de Maaijer-Gielbert, C. Gu, Á. Somogyi, V.H. Wysocki, P.G. Kistemaker, T.L. Weeding, J. Am. Soc. Mass Spectrom. 10 (1999) 414.
[34] X.-J. Tang, P. Thibault, R.K. Boyd, Anal. Chem. 65 (1993) 2824.
[35] J.L. Jones, A.R. Dongré, Á. Somogyi, V.H. Wysocki, J. Am. Chem. Soc. 116 (1996) 8368.
[36] J.L. Stephenson Jr., S.A. McLuckey, J. Am. Chem. Soc. 118 (1996) 7390.
[37] S.A. McLuckey, J.L. Stephenson Jr., Mass Spectrom. Rev. 17 (1998) 369.
[38] J.L. Stephenson Jr., S.A. McLuckey, Anal. Chem. 70 (1998) 3533.
[39] G.J. Van Berkel, G.L. Glish, S.A. McLuckey, Anal. Chem. 62 (1990) 1284.
[40] S.A. McLuckey, D.E. Goeringer, G.L. Glish, J. Am. Soc. Mass Spectrom. 2 (1991) 11.
[41] J.N. Louris, J.S. Brodbelt-Lustig, R.G. Cooks, G.L. Glish, G.J. Van Berkel, S.A. McLuckey, Int. J. Mass Spectrom. Ion Processes 96 (1990) 117.
[42] S.A. McLuckey, G.L. Glish, G.J. Van Berkel, Int. J. Mass Spectrom. Ion Processes 106 (1991) 213.
[43] K.J. Hart, S.A. McLuckey, J. Am. Soc. Mass Spectrom. 5 (1994) 250.
[44] A. Colorado, J. Brodbelt, J. Am. Soc. Mass Spectrom. 7 (1996) 1116.
[45] K.G. Asano, D.E. Goeringer, S.A. McLuckey, Int. J. Mass Spectrom. 185/186/187 (1999) 207.
[46] D.E. Goeringer, K.G. Asano, S.A. McLuckey, Int. J. Mass Spectrom. 182/183 (1999) 275.
[47] J.L. Stephenson Jr., S.A. McLuckey, Int. J. Mass Spectrom. Ion Processes 162 (1997) 89.
[48] R.E. Kaiser Jr., R.G. Cooks, J. Moss, P.H. Hemberger, Rapid Commun. Mass Spectrom. 3 (1989) 50.
[49] T.A. Whitney, L.P. Klemann, F.H. Field, Anal. Chem. 43 (1971) 1048.